New Materials, Compounds and Applications
Vol.9, No.3, 2025, pp.601-610
https://doi.org/10.62476/nmca.93601

EFFECT OF GAMMA IRRADIATION ON ELECTRICAL PROPERTIES OF THIN FILM HETEROJUNCTION BASED ON CdMnSe

M.A. Mehrabova[1,2*], N.I. Huseynov[2], R.M. Sadigov[1,3,4], A.M. Nazarov[4], A.A. Abdullayeva[1], A.I. Kazimova[5]

[1]Azerbaijan Technical University, Baku, Azerbaijan
[2]Institute of Radiation Problems, Ministry of Science and Education, Baku, Azerbaijan
[3]Azerbaijan State University of Economics, Baku, Azerbaijan
[4]Institute of Physics, Ministry of Science and Education, Baku, Azerbaijan
[5]Ganja State University, Ganja, Azerbaijan

Abstract. The fabrication conditions for $CdSe/Cd_{1-x}Mn_xSe$ thin-film heterojunctions were established. The crystal structure and surface morphology of the thin films were examined. It was found that the $Cd_{1-x}Mn_xSe$ (x = 0.15) thin film crystallizes in a sphalerite-type cubic structure with a lattice parameter of a = 6.05 Å and that Mn atoms are uniformly incorporated into the CdSe lattice without the formation of secondary phases at the microscale. Optical spectra were analyzed and the corresponding band gaps were determined: Eg = 1.74 eV for CdSe and Eg = 1.65 eV for $Cd_{1-x}Mn_xSe$ (x = 0.15). To investigate the current transport mechanism, current-voltage characteristics were measured, including the influence of γ-irradiation on these characteristics. The experiments demonstrated that the I–V behavior of the CdSe/CdMnSe heterojunction varies with the γ-irradiation dose. These changes are primarily attributed to the creation of defects and recombination centers in the crystal lattice induced by irradiation, as well as to a reduction in carrier mobility. Relaxation processes were also studied. The fast relaxation component (τ = 15-35 μs) was associated with intrinsic transitions, whereas the slow relaxation component (τ = 100-200 μs) was related to impurity excitation and exhibited dependence on the irradiation dose. The energy levels of radiation-induced defects responsible for photoconductivity were identified within the range of 0.17-0.22 eV, with defect concentrations on the order of 10^{13}-10^{15} cm^{-3}.

Keywords: *Heterojunction, thin films, semimagnetic semiconductors, current-voltage characteristics, lifetime, relaxation.*

Corresponding Author: *M.A. Mehrabova, Azerbaijan Technical University; Institute of Radiation Problems, Ministry of Science and Education, Baku, Azerbaijan, Tel.: +994507318177, e-mail: metanet.mehrabova@aztu.edu.az*

Received: *14 August 2025;* ***Accepted:*** *20 October 2025;* ***Published:*** *4 December 2025.*

1. Introduction

Modern research in semiconductor electronics is increasingly focused on the development of functional materials for alternative energy, particularly photovoltaics. In this context, heterostructures with high efficiency converting of solar energy to electristity are of special interest (Luceño-Sánchez *et al.*, 2019; Paranthaman *et al.*, 2016). In recent years, low-dimensional semiconductor structures have attracted the attention of many scientific centers (Silva *et al.*, 2012; Badera *et al.*, 2008; Munde *et al.*, 2018; Dargad, 2015; Mali *et al.*, 2021; Gonullu & Kose, 2017; Nwori *et al.*, 2021; Scragg *et al.*, 2012). One such promising research object is the CdSe/CdMnSe heterojunction, which combines the optoelectronic properties of the conventional semiconductor CdSe with those of the diluted magnetic semiconductor CdMnSe.

Heterostructures based on CdSe and CdMnSe are characterized by an optimal band gap (~1.74-2.0 eV), close to the ideal value for solar cells, as well as a high absorption coefficient of solar radiation (Nuriyev *et al*., 2019; Scarpulla *et al*., 2023). The introduction of manganese ions into the CdSe lattice makes it possible to significantly modify the electronic structure, as well as the electrical and magnetic properties of the material. In addition, the presence of magnetic ions Mn^{2+} in CdMnSe provides additional opportunities for controlling electronic and spin states, which can be useful in designing new types of highly efficient and functional photovoltaic devices, including flexible and multilayer solar panels.

In our previous works the optical properties, electronic band structure, recombination processes of charge carriers in thin films of semimagnetic semiconductors $Cd_{1-x}Mn_xSe$ were investigated (Mehrabova *et al*., 2020, 2024; Mehrabova & Mekhrabov, 2023). In this work, we first investigated CdSe/CdMnSe heterojunctions electrical properties as current-voltage characteristics, conductivity and nature of charge carriers, as well as effect of γ-irradiation on electrical properties of the CdSe/CdMnSe thin film heterojunction.

2. Methodology of the experiment

CdSe/$Cd_{1-x}Mn_xSe$ (x = 0.15) thin film heterojunction was grown on a glass substrate with a conduction SnO_2 layer by molecular beam condensation (MBC) method in a УВН-71-P3 vacuum installation in a vacuum of 10^{-4} Pa (Mehrabova & Mekhrabov, 2023; Nuriyev *et al*., 2019; Mehrabova *et al*., 2020; Antoszewski & Pecold, 1980; Dargad, 2015).

Glass was chosen as the substrate due to its low cost and promising applicability. As source materials, pre-synthesized CdSe compounds and solid solutions of $Cd_{1-x}Mn_xSe$ (x = 0.15) were used, which were evaporated from a graphite Knudsen cell. The evaporator temperature was optimized to ensure a sufficiently high evaporation rate while minimizing partial decomposition of the evaporated material. An additional selenium vapor source was employed to compensate for the volatile Se component lost during partial decomposition in the evaporation process. As a result, the vapor composition closely corresponded to that of the source material.

The distance between the evaporator and the substrate was fixed at 10 cm. This was chosen so that, even when the evaporator was heated to its maximum temperature (T_{sour} = 1200 K), it would not significantly affect the substrate temperature, while ensuring a uniform film thickness across the substrate surface.

The temperatures of the substrate, evaporator and additional source were controlled using platinum-rhodium thermocouples and regulated by BPT-3 instrument with an accuracy of ±0.5°C.

The crystal structure and lattice parameters as well as chemical composition of the synthesized source materials used for film growth and thin films were examined by X-ray diffraction methods using an X-ray diffractometer (XRD Advance D8, Bruker, Germany). Surface morphology was studied by scan electron microscopy (SEM) on Jeol JSM-6610LV Series SEM.

During the growth process, a thin n-CdSe layer with a thickness of d = 1.5 μm was first deposited onto a glass substrate (thickness d = 1 mm) coated with a conductive SnO_2 layer (thickness d = 0.2-0.3 μm). Subsequently, a p-$Cd_{1-x}Mn_xSe$ (x = 0.15) layer with a thickness of d = 6 μm was deposited on CdSe layer. The optimal deposition conditions were determined as follows: for n-CdSe, T_{sour} = 1100-1200 K, condensation rate υ = 15-17 Å/s and substrate temperature T_{sub} = 643–673 K; for p-$Cd_{1-x}Mn_xSe$, T_{sour} = 1100-1200 K, condensation rate υ = 18–20 Å/s and substrate temperature T_{sub} = 473-523 K. Under these conditions, structurally perfect epitaxial films oriented along the (111) plane of the cubic face-centered lattice were obtained. It should be noted that at a substrate temperature T_{sub} = 673 K, epitaxial n-CdSe films were formed, whereas at lower substrate temperatures ($T_{sub} \approx 473$ K), the crystalline structure exhibited a polycrystalline phase.

Typically, the fabrication of heterojunctions is complicated by the formation of surface defects, which significantly reduce device performance. To minimize these effects, the heterojunctions were fabricated in a single technological cycle without breaking vacuum.

For heterojunctions prepared on glass substrates, ohmic contacts were formed by vacuum deposition of nickel (Ni) films (thickness d = 2 μm). These were applied both to the conductive SnO_2 layer (on glass, at the edges) and to the n-CdSe layer (on top). Ni was selected as the contact material due to its suitable work function alignment. The type of conductivity was determined by the t.e.m.f.

The optical and electrical properties of the fabricated heterojunctions were studied. It is well known that the investigation of the electrical properties of heterojunctions is of great importance, since knowledge of the current-voltage dependence under applied external bias makes it possible to evaluate their suitability for device applications, in particular for the development of high-efficiency solar cells.

To examine the charge transport mechanism in the n-CdSe/p-$Cd_{1-x}Mn_xSe$ heterojunctions, current-voltage characteristics (VAC) were measured at room temperature. The VAC were obtained using the standard voltmeter-ammeter method under direct and reverse current conditions.

3. Results and Discussions

All diffraction peaks in the X-ray diffraction (XRD) patterns of $Cd_{1-x}Mn_xSe$, x=0.15 confirm that thin film has a sphalerite-type cubic structure with a lattice parameter of a = 6.05 Å (Figure 1).

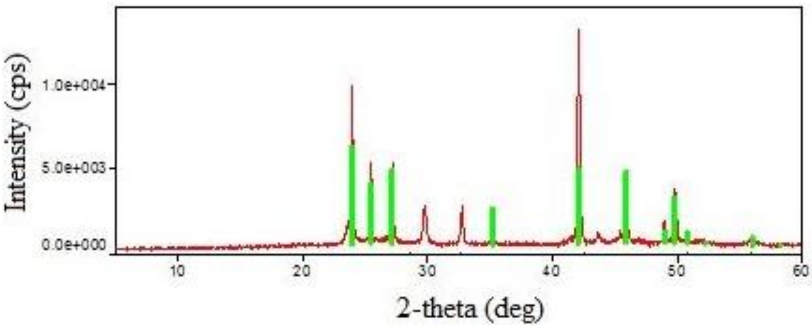

Figure 1. XRD patterns of $Cd_{1-x}Mn_xSe$, x=0.15

The surface morphology and content of $Cd_{1-x}Mn_xSe$ (x=0.15) thin films were determined by SEM method (Figure 2). The presented image shows the EDS elemental distribution map of the $Cd_{0.85}Mn_{0.15}Se$ thin film. The bright dots correspond to X-ray signals generated by the presence of characteristic elements within the scanned region.

The relatively uniform distribution of bright spots across the image suggests a homogeneous elemental composition of Cd, Mn and Se throughout the film.

No evidence of large-scale phase separation or clustering of Mn was observed, which indicates that Mn atoms are well incorporated into the CdSe lattice without forming secondary phases at the microscale. This uniform distribution is essential for stabilizing the semiconductor solid solution and maintaining consistent optical and electrical properties across the film surface.

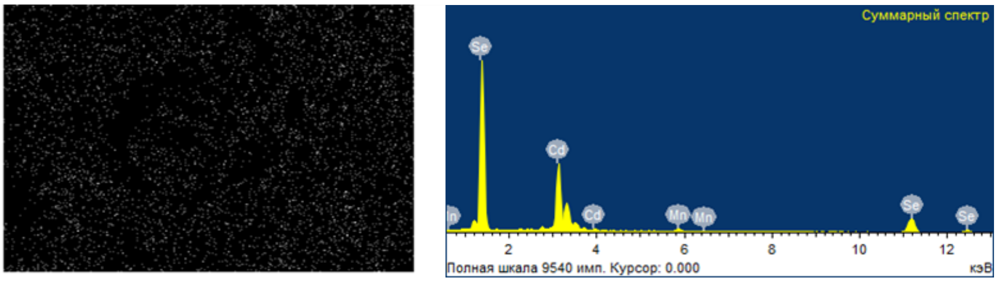

a) b)

Element	Volume %	Atomic %
Mn	1.55	2.53
Se	56.59	64.14
Cd	41.86	33.33
Result	100.00	

c)

Figure 2. Surface morphology (a) and EDX analysis (b) of $Cd_{1-x}Mn_xSe$ (x=0.15) (c) content

The combination of SEM (surface morphology) and EDS mapping (elemental distribution) confirms that the films are polycrystalline, compositionally homogeneous and free of significant impurities or segregated phases. Such uniformity supports the reliability of the optical band gap values and the electrical characteristics obtained in this study.

The optical properties of the grown heterojunction layers were investigated using a SPECORD 210 PLUS UV–Vis spectrometer (Figure 3). The absorption spectra were recorded in the wavelength range of 300-900 nm. From the absorption edge, the band gap energy was determined by plotting $(\alpha h\nu)^2$ versus photon energy ($h\nu$) and extrapolating the linear region of the curve to the energy axis (Antoszewski & Pecold, 1980). It was found that the band gap of $Cd_{1-x}Mn_xSe$ (x = 0.15) is E_g = 1.65 eV. This value is less than**,** the band gap of pure CdSe ($E_g \approx$ 1.74 eV) (Gremenok *et al.*, 2013; Mehrabova *et al.*, 2020). Such behavior can be attributed to several factors: incomplete substitution of Cd by Mn, structural disorder in the solid solution or the presence of defect states, all of which may reduce the effective optical band gap.

The obtained result suggests that, in the present growth conditions, Mn incorporation leads to a decrease in the band gap. Nevertheless, the material retains strong absorption in the visible spectral region, confirming its suitability for heterojunction optoelectronic applications such as photodetectors and solar cells.

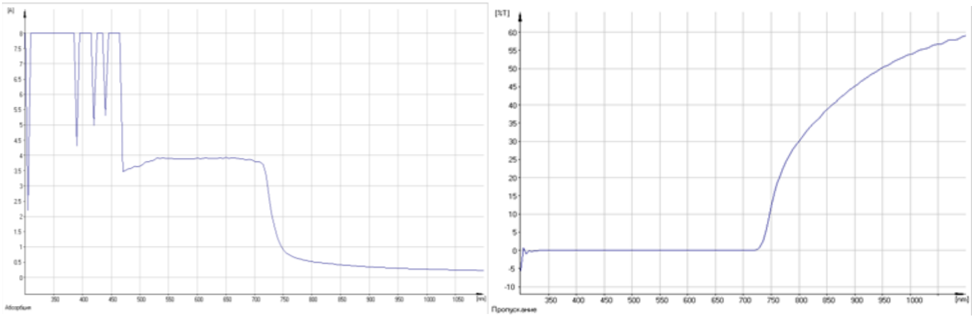

a) b)

Figure 3. Optical spectra of $Cd_{1-x}Mn_xSe$ (x=0.15) a) absorption, b) transmittion

The VAC of the n-CdSe/p-$Cd_{1-x}Mn_xSe$ heterojunction and the effect of γ-irradiation (at doses up to $D_\gamma \leq 1800$ Gy) have been investigated (Figure 4). The fact that the direct current exceeds the reverse current by the seven times at 3 V, that indicates to the formation of a heterojunction in the sample.

It should be noted that irradiation of the crystal leads to the formation of radiation-induced defects, which are thermodynamically nonequilibrium and can significantly affect the properties of $Cd_{1-x}Mn_xSe$, particularly its electrical characteristics (Mehrabova & Mekhrabov, 2023). The main types of radiation defects include vacancies, interstitial atoms and Frenkel pairs.

The irradiation of the samples with γ-quanta was performed using a 60Co (cobalt-60) gamma-ray source with a dose rate of P = 1.2 Gy/s. The exposure conditions were carefully controlled to ensure uniform irradiation of the samples throughout the process at 300 K. During irradiation, the crystals were cooled with nitrogen vapor and their temperature did not rise above 290 K.

Figure 4 shows the variation of the VAC of the CdSe/CdMnSe heterojunction depending on the γ-irradiation dose. These changes are mainly attributed to the formation of defects and recombination centers in the crystal lattice as a result of irradiation, as well as to the reduction in carrier mobility.

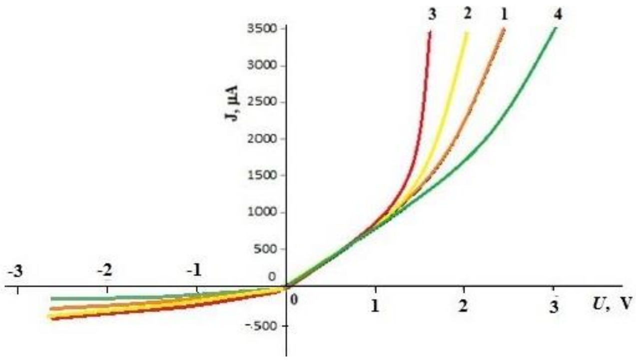

Figure 4. VAC of CdSe/$Cd_{1-x}Mn_xSe$ (x=0.15) heterojunctions: 1- D_γ =0; 2- D_γ =200 Gy; 3- D_γ =800 Gy; 4- D_γ =1800 Gy

Before irradiation, the highest conductivity, with an exponential increase of current under forward bias and very small leakage under reverse bias is observed. After irradiation with a dose of D_γ = 200 Gy, defect centers appear, leading to a slight reduction of forward current and a minor increase in leakage. After irradiation with D_γ = 800 Gy, stronger degradation is observed: the forward current decreases significantly, the exponential diode-like behavior weakens and reverse leakage increases. After irradiation with D_γ = 1800 Gy, the crystal structure is severely damaged, radiation defects dominate, the current is significantly reduced and almost no sharp increase is observed in the forward direction. Thus, increasing γ irradiation dose leads to the degradation of the CdSe/CdMnSe heterojunction: forward current decreases, reverse leakage increases and the device gradually loses its diode-like behavior.

To determine the recombination mechanism, the parameters of recombination centers and the processes of electronic transitions in the CdSe/$Cd_{1-x}Mn_xSe$ heterojunction, we employed a set of steady-state and kinetic investigation methods (Mehrabova *et al*., 2024). To obtain kinetic characteristics, the semiconductor was illuminated with short light-emitting diode pulses ($t \sim 10^{-6}$ s). The photoelectric signal, caused by the change in semiconductor potential under pulsed illumination, was preliminarily amplified by a broadband transistor amplifier, then fed into the input of an oscilloscope and recorded by a computer. The temporal resolution of the detection circuit was no worse than 10^{-8} s, which made it possible to register signals in the time interval 10^{-8}-10^{-2} s (Figure 5).

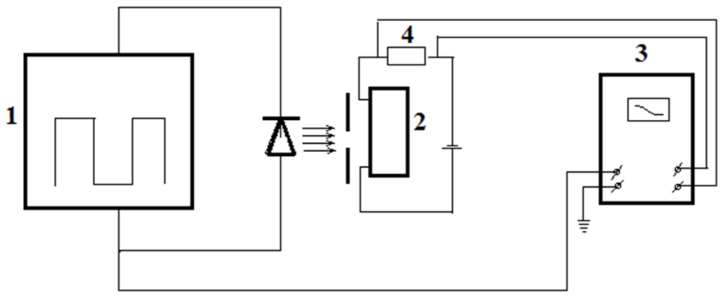

Figure 5. Block diagram of the installation for measuring the kinetics of the photoelectric effect: 1 - Generator; 2 - cell; 3 - amplifier with polarization unit; 4 - oscillography

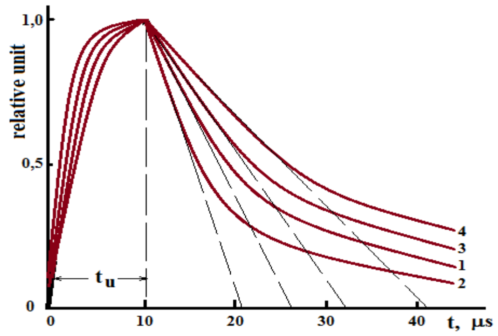

Figure 6. Kinetics of photoconductivity relaxation in $Cd_{1-x}Mn_xSe$ excited by rectangular light pulses at different γ-irradiation doses at room temperature. 1- D_γ =0; 2- D_γ =200 Gy; 3- D_γ =800 Gy; 4- D_γ =1800 Gy

Figure 6 shows the photocurrent relaxation curve in $Cd_{1-x}Mn_xSe$. The study of nonequilibrium photoconductivity relaxation curves under laser irradiation also confirms the presence of two recombination channels in $Cd_{1-x}Mn_xSe$: intrinsic and impurity-related (photocurrent relaxation occurs through fast and slow recombination channels). The fast relaxation time (τ = 15-35 μs), depending on the irradiation dose, is associated with intrinsic transitions, while the slow relaxation time (τ = 100-200 μs) is attributed to impurity excitation.

All these studies clearly demonstrated that in the $CdSe/Cd_{1-x}Mn_xSe$ heterojunction, various types of recombination centers play a primary role in the recombination processes: fast (s-type) and slow (r-type) centers. Under pulsed illumination, the carrier lifetime was determined from the kinetic decay of the photocurrent.

The possibility of estimating the lifetime of nonequilibrium charge carriers in the surface layer containing defects is considered. In the presence of multiple recombination types, the effective carrier lifetime can be determined using the following expression:

$$\frac{1}{\tau_{eff}} = \sum_i \tau_i$$

It should be noted that the surface recombination velocity in the $CdSe/Cd_{1-x}Mn_xSe$ heterojunction is a parameter characterizing the intensity of charge carrier recombination at the surface of the semiconductor sample. It is expressed in cm/s and indicates the rate at which charge carriers (electrons and holes) recombine at the sample surface, i.e., disappear as a result of mutual interaction. The higher the surface recombination velocity, the faster the excess charge carriers are removed from the surface, which can negatively affect the performance of the semiconductor device.

For the $CdSe/Cd_{1-x}Mn_xSe$ heterojunction, taking into account introduced structural defects and surface effects, the effective carrier lifetime can be determined as:

$$\frac{1}{\tau_{eff}} = \frac{1}{\tau_l} + \frac{1}{\tau_s}$$

here $\frac{1}{\tau_s} = \frac{2s}{d}$; τ_l - life time, taking into account carrier recombination at structural defects in the wafer. Here, τ_s - is the surface lifetime; s - is the surface recombination velocity; and d - is the wafer thickness. Analysis of Figure 5 showed that the carrier lifetime **is** τ =30-35mks, the surface recombination velocity s = $40\frac{sm}{s}$. The most important measurements for solar cell characterization are the accurate determination of the surface recombination velocity and its relative error. In our measurements, the relative error of the surface recombination velocity, ΔS/S, did not exceed 11%. The analysis showed that the measurement error of the surface recombination velocity decreases with increasing wafer thickness and with a higher absorption coefficient of the exciting radiation. The study showed that the photocurrent decay is not monoexponential, indicating the presence of multiple recombination types. Depending on the energy states of these centers, the effective carrier lifetime ranged from 10^{-6} to 10^{-3} s (Bogatyrenko & Zinovchuk, 2011).

The study of VAC characteristics and thermally stimulated current (TSC) spectra does not provide complete information about critical parameters of trap centers, such as their energy depth, concentration, capture cross-section or the distribution of localized levels within the bandgap of the material.

Investigation of recombination processes is an essential step in studying the physical properties of semiconductor materials and devices based on them. The mechanism of charge carrier recombination determines the behavior of photoelectric, luminescent and injection phenomena, which underlie most practical applications of semiconductors. In this work, we investigate the recombination processes of charge carriers, as well as the effect of γ-radiation on these processes.

The dose dependence of carrier lifetime in the range 0-1800 Gy exhibits a maximum and then decreases. The sensitive region is 0-800 Gy, which can be explained by an increase in the degree of system ordering. At doses above 800 Gy, defect formation leads to a noticeable reduction in the number of r-type centers responsible for photosensitivity, resulting in a sharp decrease in carrier lifetime.

In irradiated $Cd_{1-x}Mn_xSe$ samples, at low doses (up to 1000 Gy), the photosensitivity changes only slightly, which is due to the high density of structural defects in the initial crystals. With increasing γ-irradiation dose up to 1800 Gy, the photosensitivity of the samples increased, while above 1000 Gy it decreased (Figure 7).

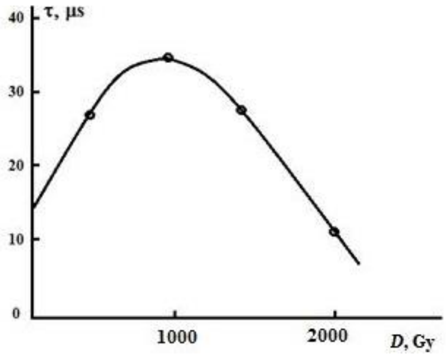

Figure 7. Dose dependence of the charge carrier lifetime in the $CdSe/Cd_{1-x}Mn_xSe$ heterojunction

The radiation-induced changes in photosensitivity are caused both by the alteration of nonequilibrium hole lifetimes due to the restructuring of defects in the crystal bandgap and changes in the concentration of photosensitivity centers, as well as by the filling of these centers with holes. The energy position of radiation defects responsible for photoconductivity was 0.17-0.22 eV and their concentration ranged from 10^{13} to 10^{15} cm^{-3}.

Thus, the study of the photoelectric characteristics of the samples showed that defect formation under γ-irradiation leads to significant changes in the concentration of localized levels, including n-type photosensitivity centers.

The obtained results allow for the assessment of the potential use of the $CdSe/Cd_{1-x}Mn_xSe$ heterostructure as an active component in next-generation flexible solar cells.

4. Conclusion

The conditions for obtaining $CdSe/Cd_{1-x}Mn_xSe$ heterojunctions were determined. The crystal structure and surface morphology of the resulting samples were investigated. It was defined that $Cd_{1-x}Mn_xSe$ thin film has a sphalerite-type cubic structure with a lattice parameter of a = 6.05 Å and Mn atoms are well incorporated into the CdSe lattice without forming secondary phases at the microscale.

The optical spectra were studied and the bandgap widths were determined: for CdSe, E_g = 1.74 eV; for $Cd_{1-x}Mn_xSe$ (x = 0.15), E_g = 1.65 eV, which is consistent with our theoretical results and literature data.

To study the current transport mechanism in the heterojunction, the VAC’s were investigated at room temperature, as well as the effect of γ-irradiation on these characteristics. Experiments show the variation of the VAC of the CdSe/CdMnSe heterojunction depending on the γ-irradiation dose. These changes are mainly attributed to the formation of defects and recombination centers in the crystal lattice as a result of irradiation, as well as to the reduction in carrier mobility.

Under pulsed illumination, the carrier lifetime was determined from the kinetic decay of the photocurrent. The study of nonequilibrium photoconductivity relaxation curves under laser irradiation confirms the presence of two recombination channels - intrinsic and impurity-related - in the $CdSe/Cd_{1-x}Mn_xSe$ heterojunction. Photocurrent relaxation occurs through fast and slow recombination channels. The fast relaxation time (τ = 15-35 μs) is associated with intrinsic transitions, while the slow relaxation time (τ = 100-200 μs) is due to impurity excitation and depends on the irradiation dose.

The radiation-induced changes in photosensitivity are caused both by the alteration of nonequilibrium hole lifetimes due to the restructuring of defects in the crystal bandgap and changes in the concentration of photosensitivity centers, as well as by the filling of these centers with holes. The energy position of the radiation defects responsible for photoconductivity was 0.17-0.22 eV, with concentrations ranging from $10^{13}$to 10^{15} cm^{-3}.

Thus, the study of the photoelectric characteristics of the $CdSe/Cd_{1-x}Mn_xSe$ heterojunction showed that defect formation under γ-irradiation leads to a significant change in the concentration of localized levels.

References

Antoszewski, J., Pecold, E.K. (1980). Fundamental optical properties of $Cd_{1-x}Mn_xSe$ single crystals. *Solid State Communications, 34*(9), 733-735.

Badera, N., Godbole, B., Srivastava, S.B., Vishwakarma, P.N., Chandra, L.S., Jain, D. & Ganesan, V. (2008). Photoconductivity in $Cd_{1-x}Mn_xS$ thin films prepared by spray pyrolysis technique. *Solar Energy Materials and Solar Cells, 92*(12), 1646-1651.

Bogatyrenko, V. V., & Zinovchuk, A. V. (2011). Measurement of the rate of surface recombination and the volume lifetime in Si plates according to the kinetics of excess heat radiation. *Fizika i tekhnika poluprovodnikov, 45*(1), 62-66.

Dargad, J.S. (2015). Preparation of $Cd_{1-x}Mn_xSe$ DMS thin films by CBD: Studies on optical and electrical properties. *International Journal of Applied Research (IJAR), 1*(10), 926-932.

Gonullu, M.P., Kose, S. (2017). On the role of high amounts of Mn element in CdS structure. *Metallurgical and Materials Transactions A, 48*(3), 1321-1320.

Gremenok, V.F., Zalessky, V.B., Mursakulov, N.N. & Tivanov, M.S. (2013). *Thin-Film Solar Cells Based on Cu(İn,Ga)(Se,S)2 Semiconductor Materials with a Chalcopyrite Structure*. Baku, Elm, 252.

Luceño-Sánchez, J.A., Díez-Pascual, A.M. & Peña Capilla, R. (2019). Materials for photovoltaics: State of art and recent developments. *International Journal of Molecular Sciences, 20*(4), 976.

Mali, A.E., Gaikwad, A.S., Borse, S.V. & Ahire, R.R. (2021). Influence of Mn^{2+} magnetic ions on the properties of $Cd_{1-x}Mn_xS$ thin films synthesized by chemical bath deposition. *Journal of Nano- and Electronic Physics, 13*(1), 01004-5.

Mehrabova, M.A., Huseynov, N.I., Asadullayeva, S.G., Nazarov, A.M., Poladova, V.N. & Suleymanli, S.P. (2024). Photoelectrical properties of CdMnSe. *Advanced Physical Research, 6*(3), 206-210.

Mehrabova, M.A., Mekhrabov, A.O. (2023). Effect of gamma irradiation on electrical and photoelectrical properties of $Cd_{1-x}Mn_xTe$ thin films. *Machine Science,* 2, 70-77.

Mehrabova, M.A., Orujov, H.S., Hasanov, N.H., Kazimova, A.I. & Abdullayeva, A.A. (2020). Ab initio calculations of defects in CdMnSe semimagnetic semiconductors. *Mechanics of Solids, 55*(1), 108-113.

Munde, B.S., Mahewar, R.B. & Ravangave, L.S. (2018). Study of spectroscopic properties of $Cd_{0.6}Mn_{0.4}S$ chemical bath deposited thin film for solar cell applications. *International Journal of Research and Analytical Reviews*, *5*(3), 962-966.

Nuriyev, I.R., Mehrabova, M.A., Nazarov, A.M., Hasanov, N.H., Sadigov, R.M., Farzaliyev, S.S. & Farajov, N.V. (2019). Structure and surface morphology of $Cd_{1-x}(Mn,Fe)_xSe$ epitaxial films. *Journal of Surface Investigation: X-ray, Synchrotron and Neutron Techniques*, *13*(6), 1083-1085.

Nwori, A.N., Ezenwaka, N.L., Ottih, I.E., Ngozi, A.O. & Okoli, N.L. (2021). Study of the optical, electrical, structural and morphological properties of electrodeposited lead manganese sulphide (PbMnS) thin film semiconductors for possible device applications. *Journal of Modern Materials*, *8*(1), 40-51.

Paranthaman, M.P., Wong-Ng, W. & Bhattacharya, R.N. (2016). *Semiconductor Materials for Solar Photovoltaic Cells,* 218. Switzerland: Springer International Publishing.

Scarpulla, M.A., McCandless, B., Phillips, A.B., Yan, Y., Heben, M.J., Wolden, C. & Hayes, S.M. (2023). CdTe-based thin film photovoltaics: Recent advances, current challenges and future prospects. *Solar Energy Materials and Solar Cells*, 255, 112289.

Scragg, J.J., Dale, P.J., Colombara, D. & Peter, L.M. (2012). Thermodynamic aspects of the synthesis of thin-film materials for solar cells. *ChemPhysChem*, *13*(12), 3035-3046.

Silva, R.D., Neto, E.D.F., Dantas, N.O. & Neralla, S. (2012). Optical, magnetic and structural properties of semiconductor and semimagnetic nanocrystals. *Nanocrystals - Synthesis, Characterization and Applications*, 1, 62-80.